THE EFFECT ON THRUST AND EFFICIENCY OF AN UPSTREAM KARMAN WAKE ON AN OSCILLATING FOIL

D.N. Beal, F.S. Hover, and M.S. Triantafyllou
Department of Ocean Engineering
Massachusetts Institute of Technology

Cambridge, MA 02139 USA
dnbeal@mit.edu

1 Abstract

The performance of an oscillating hydrofoil moving in heave and pitch was studied while interacting with the wake shed by an upstream, oscillating D-cylinder. The interaction between the foil and the oncoming vortex street can be changed by altering the phase of the foil heave motion relative to that of the cylinder heave trajectory. With the foil oscillating frequency fixed to that of the cylinder, experimental parameters varied include separation distance between the foil and cylinder, heave amplitudes of the foil and cylinder, and the maximum angle-of-attack of the foil relative to the instantaneous flow velocity. At low angles-of-attack, the effect of the vortex wake was most acute, with efficiencies seen as high as 95%, and variations in the coefficient of thrust and efficiency with respect to the foil / cylinder phase seen as high as 0.5 and 25%, respectively. The foil / vortex interaction mode, as well as the condition of the combined foil / cylinder wake, were identified by injecting dye into the flow in front of the cylinder. High performance was found to occur when the foil intercepts the wake vortices, and poor performance was seen when the foil was set to avoid them.

2 Introduction

Throughout history, humans have marveled at the relative ease with which fish and birds can move and maneuver. Many swimming and flying animals essentially use unsteady foils, moving in two or three degrees of freedom, to produce the thrust and maneuvering forces required for their needs. In many cases a foil thruster is exposed to a non-uniform, oscillating flow, such as the rear wing of the dragonfly within the wake of the forward wing, or a fish drafting behind an obstacle in a current.

Unsteady foil-based propulsion has attracted considerable attention in the scientific community for its ability to produce high thrust and maneuvering forces [3] [7], which would enable a vehicle equipped with unsteady foil propulsors to be more capable of surviving in dangerous environments, such as tricky currents or surf. However, implementation of flapping foil technology in such environments requires control strategies specialized to detect and react to non-uniform or unsteady incoming flows. The ability to optimally react to an oncoming vortex street, such as one produced by the drag wake of a body or an upstream propulsor, may allow for improved performance or recovery of energy from the wake [8].

Unsteady foils produce thrust through the creation of a 'reverse' Karman vortex street, similar to a classic drag wake but with the vortices and mean flow having the opposite sign, creating a thrust jet away from the propulsor. Triantafyllou [9], Anderson [2], and Read [7], have shown unsteady foils to be capable propulsors within certain parametric boundaries.

Two-dimensional hydrofoils moving in heave and pitch have shown heightened performance when interacting with a vortex wake, with the amount of the improvement determined by the mode of the foil's interaction with the vortices. Streitlien [8] used computational simulations of heaving and pitching foils within a Karman Street to show that efficiencies greater than 100% can occur if the foil trajectory *intercepts* the oncoming vorticity, allowing it to recover energy lost by an upstream body. When the foil was seen to be *slaloming* around the vortices, avoiding contact, the performance was relatively poor.

Others have visually noted the effect of an unsteady foil interacting with an oscillating wake. Koochesfahani & Dimotakis [6] have experimentally shown that a pitching foil can cancel the wake of an upstream foil within a shear layer. Gopalkrishnan, et. al. [4] performed a set of experiments using an oscillating, D-section cylinder within a uniform flow, with a downstream, pitching foil heaving in tandem. They found that the foil's interaction with the vortex wake influences the form of the combined foil and cylinder wake. Using kalliroscopic fluid, they identified three primary vortex patterns:

- Constructive Vortex Merging: The vortex from the cylinder merges with a like-signed vortex from the foil, creating a vigorous wake.
- Destructive Vortex Merging: Oppositely signed vortices from the cylinder and foil pair and twist into one another, eventually eliminating the weaker, yielding a less-vigorous combined wake.
- Vortex Pairing: Oppositely signed vortices from the foil and cylinder pair and together move off the flow centerline in a direction transverse to the mean foil motion, resulting in less mean wake velocity in the direction of motion

Gopalkrishnan changed the separation distance between the foil and cylinder in order to alter the interaction between the foil and the cylinder's oscillatory wake. They found that the foil thrust and efficiency were heavily dependent on the cylinder-foil separation, not only due to the changing wake strength but also due to changing the foil / vortex interaction mode.

Using Digital Particle Image Velocimetry (DPIV) Anderson [1] was able to show that the interception mode was likely to result in destructive merging, with a higher mean foil thrust. Slaloming was found to result in constructive merging, with lower mean thrust.

These previous studies did not study flow visualization and quantify performance on the same apparatus, nor was the hardware used capable of testing a wide range of parameters. The experiments described in this paper were performed on an apparatus similar to that used by Gopalkrishnan. Now, however, the foil and D-cylinder are allowed to heave independently, so while the previous work varied the foil / vortex-wake interaction mode by changing the foil / cylinder separation, the current research separates the two parameters, giving a clearer understanding of the effect of the interaction mode on the foil's measured thrust and efficiency. Using dye visualization on the same apparatus, we can then correlate the phase of peak performance with the interaction and combined wake modes identified by Streitlien and Gopalkrishnan, revealing the optimum motion strategy of a foil within a vortex wake, and giving insight into an active energy recovery device.

3 Experimental Methods

3.1 Apparatus

The hydrofoil experiments were performed using a NACA 0012 foil with a $10cm$ chord and a $60cm$ span, capable of moving in heave and pitch. The pitch pivot is located 1/3 chord from the leading edge, and is actuated using a light chain driven by an overhead motor. The foil strut is attached, through the linear heave drive, to an overhead carriage in the MIT Testing Tank Facility, as described in Read [7]. The tank has a test section with $18m$ length, $2.6m$ width, and a $1.4m$ depth. The carriage, via a computer-controlled belt drive, moves down the tank at a constant, commanded speed.

A D-shaped cylinder is mounted on a second heave drive at an alterable position upstream from the foil, as seen in Figure 1. The D-shaped cylinder was chosen for these tests because the phase of shedding is

Flow velocity	U
Cylinder diameter	D
Separation distance between foil and cylinder	σ
Foil chord length	c
Span length	s
Oscillation frequency (radians)	ω
Foil pitch angle	$\theta(t)$
Foil pitch amplitude	θ_o
Foil angle of attack	$\alpha(t)$
Maximum angle of attack	α_o
Foil heave position	$h_f(t)$
Cylinder heave position	$h_c(t)$
Foil heave amplitude	H_f
Cylinder heave amplitude	H_c
Phase between foil heave and pitch motions	ψ
Phase between foil and and cylinder heave motions	ϕ
Cylinder Strouhal number	$St_c = \frac{1}{\pi} H_c \omega / U$
Foil Strouhal number	$St_f = \frac{1}{\pi} H_f \omega / U$
Foil thrust	$T(t)$
Foil lift	$L(t)$
Foil torque	$\tau(t)$
Mean thrust coefficient	$C_t = \overline{T} / \frac{1}{2} \rho U^2 cs$
Mean power coefficient	$C_p = \frac{\overline{\left(L\frac{dh}{dt} + \tau\frac{d\theta}{dt}\right)}}{1/2 \rho U^3 cs}$
Foil Efficiency	$\eta = C_t U / C_p$
Reynolds Number	$Re = cU/\nu$

Table 1: Nomenclature

relatively constant with motion [4], and that it produces a robust wake even with objects nearby downstream. The cylinder acts exclusively as a vortex generator, and performance calculations are done without considering the cylinder as part of the system.

The motion-control computer is located on the carriage. Computer control of all motions allows a large parameter space to be explored.

As we'd like the flow to be as two-dimensional as possible, and wish to minimize end-effects, 12-inch diameter endplates are mounted to inside of the foil and cylinder struts, as shown in Figure 2, just a cou-

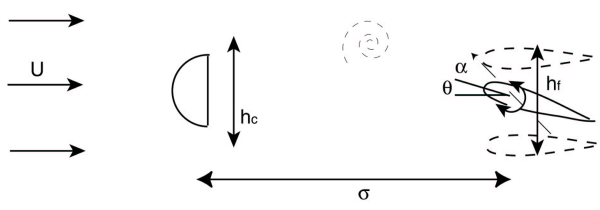

Figure 1: Diagram of the Test Setup

ple of millimeters from the ends of the foil and cylinder. For the sake of visualization the endplates were manufactured from clear Lexan.

Encoders and a potentiometer measure the positions of the heave drives and the pitch drive, respectively, and Kistler piezoelectric force sensors measure the instantaneous thrust, lift, and torque on the foil, as well as the drag and lift of the cylinder. All data is collected on a second computer, where results can be analyzed between experimental runs.

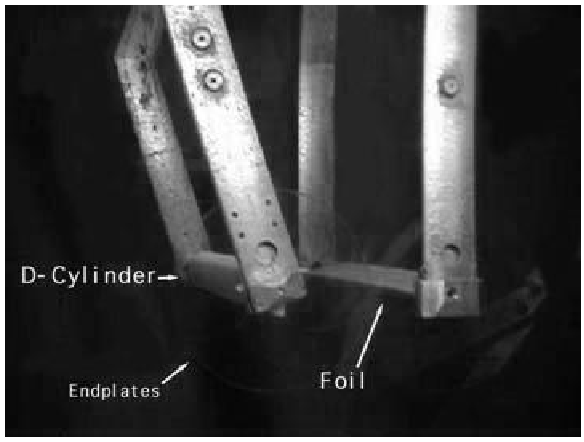

Figure 2: The foil and cylinder are mounted to the struts shown

The system can be set up to inject dye anywhere into the stream. In order to prevent the dye from dispersing too rapidly, the water-based dye was mixed with polyethylene oxide at a 100:1 mass ratio. This helps the dye hold together when injected into the flow, without adversely changing its viscosity or density.

3.2 Motion Trajectories

In order to create a strong cylinder wake, the cylinder trajectory was set to sinusoidally oscillate at its 'natural' shedding frequency, at which the cylinder would shed in a uniform flow even if not oscillating (calculated using the Strouhal number based on diameter equal to 0.20):

$$\omega = 0.20\frac{U}{D} \cdot 2\pi \tag{1}$$

$$h_c(t) = H_c \sin(\omega t + \phi) \tag{2}$$

The variable foil parameters include amplitude of heave motion, maximum angle-of-attack to the instantaneous flow velocity, phase between foil heave and pitch motions, and the phase between foil and cylinder heave motions. For obvious reasons, the foil frequency was set equal to the cylinder frequency for all trials.

The foil heave and pitch motions are nominally sinusoids. However, due to the nature of the angle-of-attack function (see eqn. 4), it is impossible to get the 0° maximum angle-of-attack profile desired for some of these experiments with pure sinusoidal motions. Hence, the heave motion profile was calculated to give a sinusoidal angle-of-attack profile, which has been found to improve efficiency [5], and also allows us to guarantee a 0° angle-of attack when necessary. The instantaneous angle-of-attack is defined as follows:

$$\theta(t) = \theta_o \sin(\omega t + \psi) \tag{3}$$

$$\alpha(t) = \arctan\left(\dot{h}_f(t)/U\right) - \theta(t) \tag{4}$$

Rearranging (4) for $h_f(t)$ and setting $\alpha(t) = \alpha_o \cos(\omega t)$ gives:

$$h_f(t) = U \int \tan\left(\alpha(t) + \theta(t)\right) dt \tag{5}$$

which, knowing the heave amplitude H_f, can be solved for h_f and θ_o iteratively.

This results in a foil heave motion profile visually similar to a sinusoid, but with a sinusoidal angle-of-attack profile, as can be seen in Figure 3 for $\alpha = 5°$, $h_f = 0.5D$.

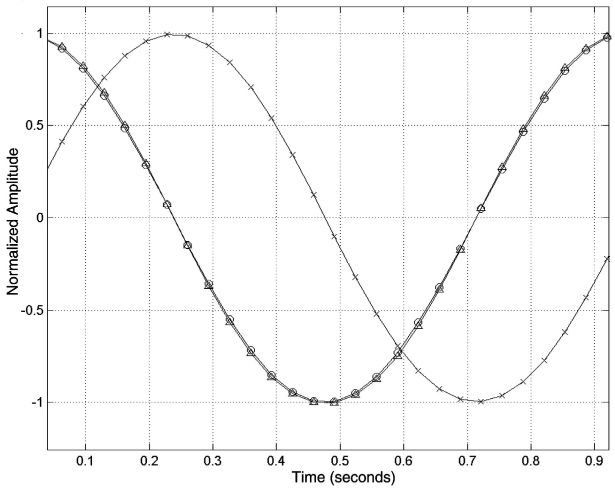

Figure 3: Trajectories of $\theta(t)/\theta_o$ (o's), $h_f(t)/H_f$ (x's), and $\alpha(t)/\alpha_o$ ($\triangle$'s)

Output power is calculated using the mean thrust and forward velocity, and input power (to calculate efficiency) is measured by multiplying the lift and torque by the instantaneous heave and pitch velocities, respectively.

Experiments were performed with 2- and 3-inch cylinders, with a cylinder / foil spacing between 3.3 and 6.0 diameters. The spacing was measured from the point of connection on the cylinder ($1/4D$ forward of the back, flat edge), to the axis of the foil (1/3 chord from the leading edge). Cylinder and foil heave amplitudes were independently varied between 0.25 and 1.0 diameters, the phase between heave and pitch was set to 90° for all tests, and α_o was varied between 0 and 25°. The phase between foil and cylinder heaves was varied between 0 and 330°, at 30° intervals, in order to explore the full range of foil / vortex interactions for each parameter set. All tests were performed at a Reynolds number of 40,000.

As the point of the experiments was to show the effect of foil / vortex interaction on performance, the tests performed were those that were expected to show that effect most clearly. At first, the foil parameters were chosen in a range found to be optimal for foil motion without the presence of the cylinder [7].

However, it was found that the vortex street had the most noticeable effect on performance when the foil-induced forces were low (ie. at low heave amplitudes and angles-of-attack). Hence, low-power trajectories were the focus of the remainder of the tests. All plots shown in this paper have 8 tests per data point, taken over the course of two days.

As it was only possible to do a couple of dye visualization runs before having to run the tank's filter to clear up the water, we only chose to visualize and photograph points of highest or lowest thrust and efficiency. A Nikon 990 digital camera was mounted next to the window at the side of the tank, and could take high-resolution photographs of the apparatus and wake as the carriage moved past. The dye was injected in the center of the span, approximately 18 inches upstream from the cylinder.

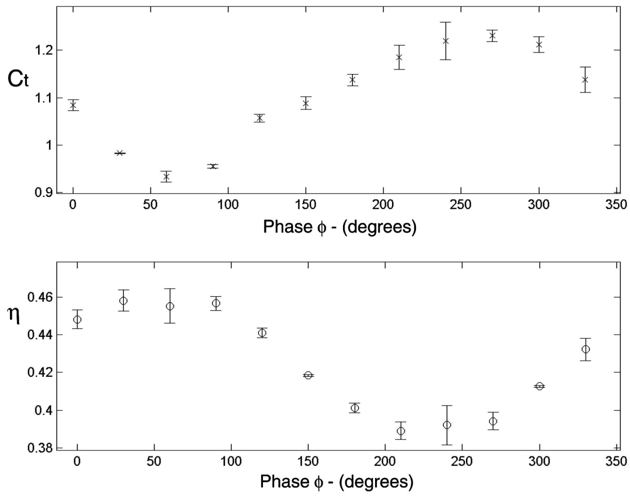

Figure 4: Thrust and Efficiency for $\sigma = 3.33D$, $\alpha_0 = 25°$, $H_f = 1.0D$, $H_c = 1.0D$, $St_f = 0.40$. Error bars represent the standard deviation of the data. Without the cylinder present, the foil was found to have $C_t = 0.9$ and $\eta = 0.43$

4 Results

4.1 Performance Experiments

When exploring the parameter space, it was found that the foil within a cylinder wake performed at thrusts and efficiencies higher than for the foil alone in steady flow. In fact, the highest efficiencies were found near zero angle-of-attack, where the foil within a uniform flow would be producing negative thrust. It should be noted that the velocity defect behind the cylinder gives the foil a slower mean incoming flow than that of the freestream, which corresponds to a higher equivalent angle-of-attack and foil Strouhal number. This incoming flow also modifies the efficiency, yielding a higher calculated efficiency due to using a higher velocity than the foil actually sees (the carriage velocity vs. the carriage velocity minus the velocity defect from the cylinder).

So although higher performance was expected because the foil was 'drafting' behind the cylinder, it was also expected to see variation in that performance depending on the foil to cylinder phase, ϕ. Higher energy runs, like those found by Read [7] to perform admirably without the presence of an upstream cylinder, were found to have a modest increase in thrust, as well as show only modest variation in thrust and efficiency with varying ϕ, as seen in Figure 4. As would be expected, the effect of vorticity was larger for smaller separation distances, σ.

Figure 4 shows that both the thrust and efficiency plots look almost sinusoidal with ϕ, with peaks in thrust corresponding with valleys in efficiency, and vice versa. Although Streitlien showed that, in general, thrust and efficiency follow each other, with peaks and valleys found at the same ϕ [8], this particular run was at a higher heave amplitude than those explored in previous studies. Experiments performed at lower heave amplitudes show better agreement with the general trends shown by Streitlien. The differing results seen in this case may involve the cylinder wake no longer being a clear '$2S$' wake, due to the high heave amplitude.

When the foil thrust and input power are low, the recovered energy from the vortex wake was found to have more relative effect. In fact, extremely high efficiencies were seen ($> 95\%$) for a low heave ($H_f = 0.5D$) and $0°$ angle-of-attack profile (see Fig-

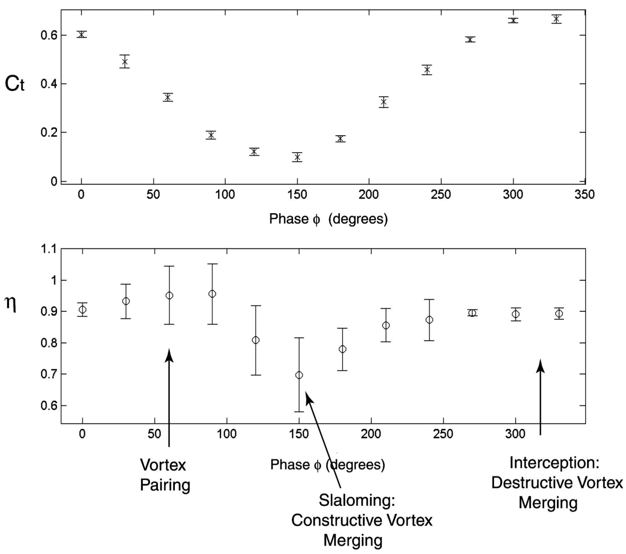

Figure 5: Thrust and Efficiency for $\sigma = 3.33D$, $\alpha_0 = 0$, $H_f = 0.5D$, $H_c = 0.4D$, $St_f = 0.20$. Error bars represent the standard deviation of the data. The interaction and combined wake modes found using visualization are also labelled.

ure 5). Efficiencies were found to be highest when the foil heave was slightly greater than that of the cylinder, likely resulting from the encountered cylinder wake being a tad wider than the peak-to-peak cylinder motion.

As seen in Figure 5, the results were seen to be highly dependent on ϕ, as the coefficient of thrust varied by 0.5 and efficiencies varied by as much as 25% depending on how the foil was moving through the cylinder's vortex wake. Although the thrust plot still looks sinusoidal with phase, the efficiency plot now exhibits a plateau behavior over most of the high thrust phase angles, with a sharp valley in the low thrust region. The peak efficiencies were seen at mediocre thrust phases ($\phi = 60 - 90°$), but this was not seen on the other side of the low-efficiency valley ($\phi = 210 - 240°$).

Figure 5 shows significant scatter in the efficiency data for the lower thrust runs. This is likely due to the experiments nearing the limits of sensitivity in the power measurements for the apparatus. The efficiency metric is built from the division of two numbers, each of which have growing *relative* error as the forces and powers become smaller. Most notably, the Kistler load cells are finicky, and exhibit drift as well as slight transient effects from 'wiggling' the lead wires that run from the sensors to the charge amplifiers, which invariably happens as the foil oscillates up and down. In fact, although higher efficiencies were seen for even smaller heave amplitudes, the scatter became unacceptably large relative to the small forces, and that data is not presented here.

4.2 Visualization

As the zero angle-of-attack runs were deemed the most interesting, all of the photographs here were taken with the foil moving in the configuration shown in Figure 5.

Figure 6 shows the foil at the phase seen to result in the highest thrust, $\phi = 330°$, and shows the foil *intercepting* the vortices shed by the cylinder. The combined wake shows little large-scale vorticity, reflecting Gopalkrishnan's Destructive Vortex Merging wake mode.

At the point of lowest thrust and efficiency, $\phi = 150°$, as shown in Figure 7, the foil is seen to be *slaloming* around the vortices, and the combined wake shows strong drag vorticity, corresponding to Constructive Vortex Merging.

A foil / cylinder phase of 60°, the point of highest efficiency but mediocre thrust, shows an interaction mode in between interception and slaloming, but exhibits Vortex Pairing in the combined wake, as shown in Figure 8.

These results agree strongly with the conclusions of Streitlien and Gopalkrishnan. As Streitlien has shown, the foil performance is highest in the interception mode, and lowest while slaloming. And as Gopalkrishnan predicted, the performance is best when the combined wake is weakest, and worst when the vorticity shed by the foil strengthens the wake vorticity.

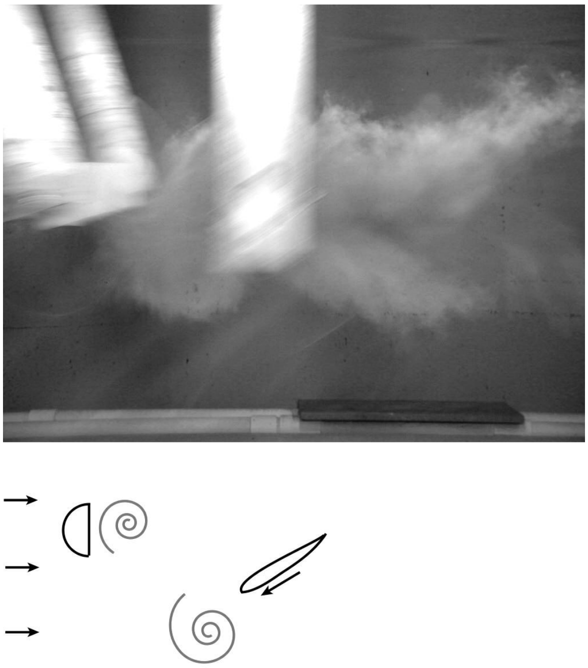

Figure 6: With the same configuration as in Figure 5, $\phi = 330°$, the foil is seen to intercept the wake vorticity, resulting in Destructive Merging, and little vorticity in the combined wake.

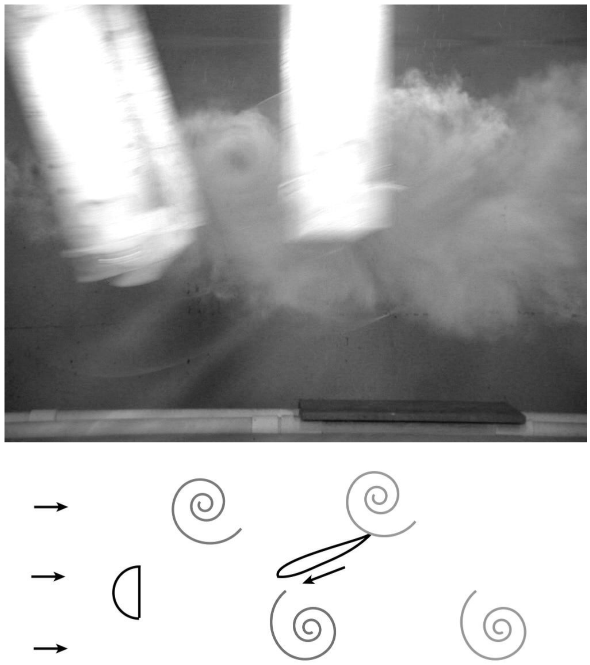

Figure 7: With the same configuration as in Figure 5, $\phi = 150°$, the foil is seen to slalom around the wake vorticity, resulting in Constructive Merging, and a vigorous combined wake.

5 Discussion & Conclusions

A general swimming strategy for a foil propulsor within a Karman wake can be summed up as 'interception is king'. The interception mode appears to give the best thrust in most cases, and although the efficiencies are slightly lower than some seen for the low angle-of-attack experiments, the interception regions exhibit considerably higher thrust with more robust efficiency.

These experiments support the earlier work regarding oscillating foils in a vortex wake performed by Streitlien and Gopalkrishnan, and strengthens their conclusions by definitively showing the performance increases and visualization on the same apparatus, and by completely separating the foil / cylinder separation distance from the foil / vortex interaction, allowing us to witness the effect of changing the interaction modes independently from any other parameters.

It has been shown here, and in previous experiments, that a hydrofoil's performance can be greatly improved when drafting within and properly tuned to the wake of an upstream body. Presumably a propulsor which is to use a vortex wake to its advantage would require a method for detecting the approaching vorticity, similar to how a fish can detect vorticity using its lateral line.

Information regarding the incoming flow velocity to the foil, as well as the flow velocities in the combined wake, would go a long way to support the conclusions of this paper. Experiments with an array of hot-wire anemometers are planned for the near future.

Figure 8: With the same configuration as in Figure 5, $\phi = 60°$, creates a combined wake exhibiting Vortex Pairing

Seeing that we have obtained results where the 100% efficiency mark is within our margin of experimental repeatability, one would have to think it would be possible to obtain values over 100%, by either increasing cylinder diameter (in order to increase the strength of the vortex wake), or by increasing the sensitivity of the sensor system, so that we could perform tests at lower heave amplitudes. We have to be careful to emphasize that efficiencies found over 100% are not breaking any thermodynamic laws: The efficiency calculation does not take into account the power injected into the water by the upstream cylinder, which is encountered by the foil in the form of a drag vortex wake. An efficiency over 100% is simply a case of the undulating foil recovering energy lost by the upstream cylinder.

ACKNOWLEDGEMENT: Support from the Office of Naval Research, Contract N00014-99-1-1082, monitored by Dr. Teresa McMullen and Dr. P. Bandyopadhyay, is gratefully acknowledged.

References

[1] J. M. Anderson. *Vorticity Control for Efficient Propulsion.* PhD Thesis, MIT, Cambridge, MA, 1996.

[2] J. M. Anderson, K. Streitlien, D. S. Barrett, M. S. Triantafyllou. *Oscillating Foils of High Propulsive Efficiency.* J. Fluid Mech. , 360:41-72, 1998.

[3] P. R. Bandyopadhyay, J. M. Castano, J. Q. Rice, R. B. Phillips, W. H. Nedderman, and W. K. Macy. *Low-Speed Maneuvering Hydrodynamics of Fish and Small Underwater Vehicles.* J. Fluids Engineering, 119:136-144, 1997.

[4] R. Gopalkrishnan, M. S. Triantafyllou, G. S. Triantafyllou, D. Barrett. *Active Vorticity Control in a Shear Flow using a Flapping Foil.* J. Fluid Mech. , 274:1-21, 1994.

[5] O. Haugsdal. *Motion Control of Oscillating Foils for Steady Propulsion and Starting Maneuvers.* Master's Thesis, MIT, Cambridge, MA, 2000.

[6] M. M. Koochesfahani, P. E. Dimotakis. *A Cancellation Experiment in a Forced Turbulent Shear Layer.* AIAA Journal, 88:3713, 1988.

[7] D. A. Read. *Oscillating Foils for Propulsion and Maneuvering of Ships and Underwater Vehicles.* Master's Thesis, MIT, Cambridge, MA, 2000.

[8] K. Streithlien, G. S. Triantafyllou, M. S. Triantafyllou. *Efficient Foil Propulsion Through Vortex Control.* AIAA Journal, Vol. 34, No. 11, 1996.

[9] G. S. Triantafyllou, M. S. Triantafyllou, M. A. Grosenbaugh. *Optimal Thrust Development in Oscillating Foils with Application to Fish Propulsion.* J. Fluids and Structures, 7:205-224, 1993.